Visual experience and subsequent sleep induce sequential plastic changes in putative inhibitory and excitatory cortical neurons

Sara J. Aton[a,b,1], Christopher Broussard[c], Michelle Dumoulin[a], Julie Seibt[a], Adam Watson[a], Tammi Coleman[a], and Marcos G. Frank[a,1]

Departments of [a]Neuroscience and [c]Psychology, University of Pennsylvania, Philadelphia, PA 19104; and [b]Department of Molecular, Cellular, and Developmental Biology, University of Michigan, Ann Arbor, MI 48109

Edited* by Terrence J. Sejnowski, Salk Institute for Biological Studies, La Jolla, CA, and approved December 12, 2012 (received for review May 14, 2012)

Ocular dominance plasticity in the developing primary visual cortex is initiated by monocular deprivation (MD) and consolidated during subsequent sleep. To clarify how visual experience and sleep affect neuronal activity and plasticity, we continuously recorded extragranular visual cortex fast-spiking (FS) interneurons and putative principal (i.e., excitatory) neurons in freely behaving cats across periods of waking MD and post-MD sleep. Consistent with previous reports in mice, MD induces two related changes in FS interneurons: a response shift in favor of the closed eye and depression of firing. Spike-timing–dependent depression of open-eye–biased principal neuron inputs to FS interneurons may mediate these effects. During post-MD nonrapid eye movement sleep, principal neuron firing increases and becomes more phase-locked to slow wave and spindle oscillations. Ocular dominance (OD) shifts in favor of open-eye stimulation—evident only after post-MD sleep—are proportional to MD-induced changes in FS interneuron activity and to subsequent sleep-associated changes in principal neuron activity. OD shifts are greatest in principal neurons that fire 40–300 ms after neighboring FS interneurons during post-MD slow waves. Based on these data, we propose that MD-induced changes in FS interneurons play an instructive role in ocular dominance plasticity, causing disinhibition among open-eye–biased principal neurons, which drive plasticity throughout the visual cortex during subsequent sleep.

GABA | striate cortex | non-REM sleep | REM sleep | critical period

Monocular deprivation (MD) during a critical developmental period shifts neuronal responses in primary visual cortex in favor of open-eye stimulation. Sleep is essential for consolidating ocular dominance plasticity (ODP) in cat visual cortex (1, 2). Specifically, post-MD sleep is required to potentiate open-eye responses in cortical neurons—a process mediated via intracellular pathways involved in long-term potentiation of glutamatergic synapses (1, 3). However, the changes in network activity (during waking experience and subsequent sleep) that mediate ODP remain unknown.

One long-standing hypothesis is that ODP is gated by the balance of excitation and inhibition in the visual cortex during the critical period. This idea is supported by findings that ODP is enhanced either by increasing GABAergic neurotransmission before the critical period (4) or by reducing GABA signaling after the critical period (5–8). It has been suggested that, during the critical period, MD itself alters the balance of excitation and feedback inhibition within the visual cortex by depressing the activity of fast-spiking (FS) interneurons (9, 10). In support of this idea, ODP is first detectable in the extragranular cortical layers [i.e., 2/3, 5, and 6 (11)], where depression of FS interneuron activity has been reported after brief MD. These layers are characterized by abundant reciprocal intralaminar connections between FS interneurons and pyramidal neurons (12, 13). In contrast, in layer 4, where ODP is initially weak or absent (11), connections between FS interneurons and pyramidal neurons can be *strengthened* by MD (14). Previous work attempted to track ODP in individual cortical neurons over time (15), but did not address the relative time course and nature of plastic changes in excitatory vs. inhibitory circuits during ODP (10, 16–18). The role for ongoing network activity in sleep (vs. waking experience) in these processes is also unknown. To address these issues, we continuously measured the activity of putative GABAergic (FS) and glutamatergic (principal) extragranular neurons in the cortex of freely behaving cats throughout waking MD and subsequent sleep.

Results

Waking MD Depresses Open-Eye Responses in FS Interneurons, Whereas Post-MD Sleep Promotes ODP in Principal Neurons. To clarify how FS and principal neuron activity changes across waking MD and subsequent sleep, we continuously recorded individual neurons in cat visual cortex near the peak of the critical period for ODP (Fig. S1). Neurons were recorded from extragranular layers [81% in layer 2/3, 19% in layers 5 and 6 (Fig. S2)] using chronically implanted stereotrodes. Recordings spanned a baseline period of sleep and wakefulness, 6 h of waking MD [or, as a control for the effects of waking alone, 6 h of normal binocular vision (No-MD controls)], and 6 h of subsequent sleep (1).

We first quantified visual responses and OD at intervals to compare plastic changes in FS and principal neurons over time. We found that in freely behaving cats, OD was unchanged in principal neurons immediately after waking MD (Fig. 1*A*), but shifted in favor of the open eye after subsequent sleep. Similarly, closed-eye and open-eye response magnitudes in principal neurons were unchanged relative to baseline after MD alone, but were significantly altered (depressed and potentiated, respectively) after post-MD sleep (Fig. 1*B*). No OD changes were present in principal neurons recorded from No-MD control animals after either waking (binocular) experience or subsequent sleep; instead, responses to stimulation of both eyes were equally enhanced after sleep (Fig. S3). These data indicate a prominent role for sleep in promoting ODP among principal neurons.

Surprisingly, FS interneurons, which showed binocular responses at baseline, displayed a shift in favor of closed-eye stimulation after waking MD, and after sleep returned to binocular responsiveness (Fig. 1*A*). This transient OD shift in favor of the closed eye among FS interneurons is similar to that reported in mice after brief (3-d) MD (10). Both closed-eye and open-eye responses were altered after MD, with closed eye responses slightly (but not significantly, $P = 0.12$) enhanced, and open-eye responses significantly reduced (Fig. 1*B*). These changes reversed after post-MD

Author contributions: S.J.A. and M.G.F. designed research; S.J.A., M.D., J.S., A.W., and T.C. performed research; C.B. contributed new reagents/analytic tools; S.J.A. analyzed data; and S.J.A. and M.G.F. wrote the paper.

The authors declare no conflict of interest.

*This Direct Submission article had a prearranged editor.

[1]To whom correspondence may be addressed. E-mail: saton@umich.edu or mgf@mail.med.upenn.edu.

This article contains supporting information online at www.pnas.org/lookup/suppl/doi:10.1073/pnas.1208093110/-/DCSupplemental.

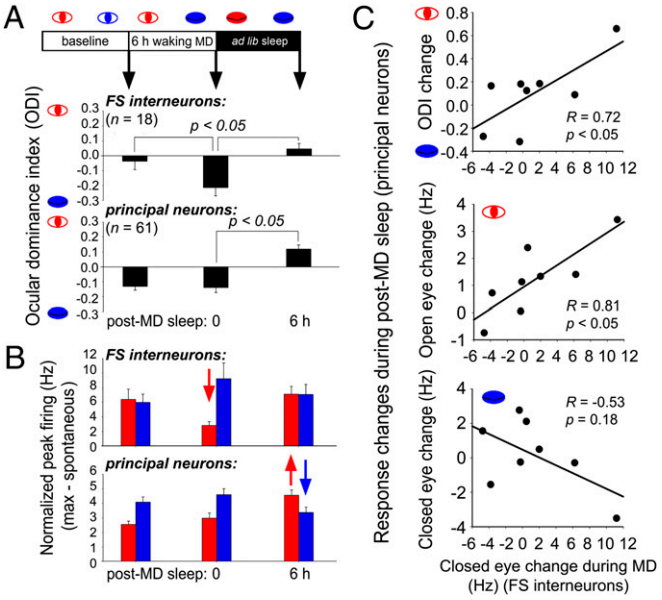

Fig. 1. Effects of visual experience and subsequent sleep on neuronal responses in freely behaving cats. (*A*) At the intervals indicated, visual responses to stimulation of the right and left eyes were compared, and ocular dominance indices (ODIs) were calculated for each neuron. An ODI of 0 indicates equal responsiveness to stimulation of either eye; ODIs of 1 and −1 indicate responsiveness to only left- or right-eye stimulation, respectively. FS interneurons showed an initial shift in favor of the closed eye after waking MD ($P < 0.05$ vs. baseline, repeated measures ANOVA), followed by a return to binocularity after subsequent sleep. Principal neurons were unchanged after waking MD, but shifted in favor of the open eye after subsequent sleep. (*B*) Open-eye responses (red) in FS interneurons were significantly depressed, and closed-eye responses (blue) were slightly enhanced, after MD; these changes were reversed, and open-eye and closed-eye responses returned to baseline levels after subsequent sleep. Open-eye and closed-eye responses in principal neurons were unchanged after waking MD alone, but were potentiated and depressed, respectively, after post-MD sleep (arrows indicate $P < 0.05$ vs. baseline, repeated measures ANOVA). (*C*) Closed-eye response changes in FS interneurons during MD correlated with subsequent plasticity in neighboring principal neurons during post-MD sleep. Values are averaged across all FS and principal neurons recorded on each stereotrode bundle ($n = 8$ recording sites at which both FS and principal neurons were recorded).

sleep (Fig. 1*B*; $P < 0.05$ after sleep vs. waking MD alone, Holm–Sidak post hoc test). Depression of visual responses was not seen after 6 h of waking under No-MD conditions where visual responses for both eyes showed a gradual enhancement, both after waking, and again after subsequent sleep (Fig. S3).

We hypothesized that MD-induced response changes in FS interneurons promote subsequent, sleep-mediated response changes in principal neurons. If this were the case, we would expect that these changes would be proportional to one another in neighboring FS and principal neuronal populations. To test this, we calculated the mean visual response change among FS interneurons at each recording site after waking MD and the mean response change among principal neurons at the same site after subsequent sleep. In cortical areas where FS interneurons showed the largest closed-eye response enhancement across MD, nearby principal neurons showed the largest plastic changes across post-MD sleep (Fig. 1*C*). This relationship supports the hypothesis that OD changes in FS interneurons during MD promote subsequent sleep-dependent changes in principal neurons.

MD-Induced Response Depression in FS Interneurons Is Consistent with Spike-Timing–Dependent Plasticity. We first examined continuously recorded data from waking MD for supportive evidence of a mechanism hypothesized to mediate initial shifts in favor of closed-eye stimulation in FS interneurons. Depression of open-eye responses during waking MD (Fig. 1*B*) could be driven by spike-timing–dependent plasticity in FS interneurons, as postulated previously (10). Coincident (±10 ms) firing between presynaptic principal and postsynaptic FS neurons within the extragranular cortex causes synaptic depression in vitro, regardless of which of the neurons fires first (19). Accordingly, the more active an excitatory input is, the greater the likelihood of both coincident FS postsynaptic activity and synaptic depression in vivo. FS interneurons in the extragranular layers receive substantial excitatory input from pyramidal neurons in the same layer [and relatively little layer 4 (12, 13, 20)]. We hypothesized that intralaminar inputs from open-eye–biased principal neurons to FS interneurons are depressed after MD, whereas inputs from principal neurons with a closed-eye bias are left intact (Fig. 2*A*).

If spike-timing–dependent plasticity mediates such changes, we would expect an increase in coincident firing between open-eye–biased principal neurons and that FS interneurons would precede response changes in FS interneurons and would be detectable at the outset of MD. To test this, we compared correlated firing in pairs of neighboring principal and FS neurons (i.e., those recorded at the same site) at baseline and immediately after inducing MD (Fig. 2*B*). In principal/FS pairs where the principal neuron was initially more biased in favor of the open eye, we found that coincident (± 10 ms) firing increased during MD (Fig. 2*C*). No similar change in coincident firing was detectable in principal/FS pairs recorded from No-MD control cats ($R = -0.23$, $P > 0.5$, for initial ocular dominance index (ODI) differential vs. coincident firing change, Pearson correlation). These changes in spike timing were present in the first hour of MD and thus preceded changes in FS interneuron responses to open-eye stimulation (detectable after 6 h of MD; Fig. 1*B*). Thus, our data support a hypothetical mechanism whereby coincident firing between FS interneurons and their open-eye–biased principal inputs during MD leads to specific depression of open-eye responses in FS interneurons.

MD-Induced Depression of FS Interneuron Activity Correlates with Sleep-Dependent ODP in Neighboring Principal Neurons. Depression of open-eye–biased excitatory inputs to FS interneurons during MD would be expected to reduce their evoked and spontaneous activity. Accordingly, feedback inhibition from FS interneurons to neighboring principal neurons would also be reduced, particularly in open-eye–biased cortical columns. To test this possibility, we first assessed the effects of MD on FS interneuron firing during waking MD and post-MD sleep, as well as on spontaneous activity (measured during blank screen presentations in visual tests). We found that firing rates for FS interneurons decreased gradually over 6 h of waking MD and remained significantly depressed, relative to baseline, for several hours post MD in all states [waking, non-rapid eye movement (NREM) sleep, and rapid eye movement (REM) sleep; Fig. 3*A*). This decrease in firing was transient (lasting roughly 6–8 h; Fig. S4) and did not occur after 6 h of waking under control (No MD) conditions (Fig. 3*A*). Instead, FS interneurons recorded from No-MD cats showed increased firing during subsequent NREM sleep ($P < 0.05$, two-way ANOVA, Holm–Sidak post hoc test). Firing during blank screen presentation was similarly depressed after MD, consistent with effects of MD in mouse visual cortex (10), but was enhanced after waking without MD (Fig. 3*C*).

We next examined whether FS interneurons with the greatest initial preference for open-eye stimulation (i.e., those that received the most open-eye–biased input at baseline) also showed the greatest reduction of firing during post-MD sleep. As shown in Fig. 3*B*, there was a significant correlation between baseline ODI and firing-rate changes, with FS interneurons that received predominately open-eye–biased input at baseline undergoing the greatest overall depression.

We then examined whether depressed FS interneuron firing was proportional to subsequent, sleep-dependent plasticity in neighboring principal neurons. We found that, in cats where FS

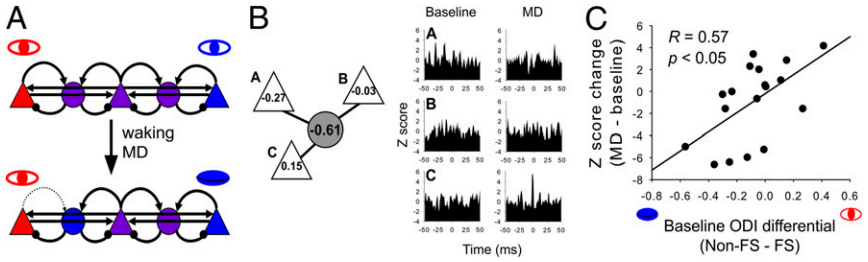

Fig. 2. MD-induced depression of open-eye responses in FS interneurons is consistent with spike-timing–dependent plasticity. (*A*) Hypothesized changes in input to FS interneurons during MD are illustrated using a simplified circuit diagram, which takes into account the columnar organization of OD preference. Principal neurons and FS interneurons are shown as triangles and circles, and excitatory and inhibitory synaptic inputs are shown as arrowheads and balls, respectively. Depression of open-eye responses could be elicited by reduction in excitatory inputs from open-eye–biased principal neurons to FS interneurons. (*B*) A group of neurons recorded at the same site (three principal neurons and a neighboring FS interneuron), with each neuron's baseline ODI. Cross-correlated firing was calculated between the FS interneuron and each principal neuron during baseline waking and in the first hour of MD. A similar analysis was carried out for each recorded FS interneuron. (*C*) In pairs of neurons where, initially, the principal neuron was more biased toward the open eye than the FS interneuron, cross-correlated firing within a ±10-ms lag increased the most during MD (calculated as a z-score change from baseline). Such an increase would be predicted to cause spike-timing–dependent depression of principal inputs to FS interneurons (19).

interneurons showed the greatest depression, principal neurons showed the greatest sleep-dependent changes in OD (Fig. 3*D*). To verify this relationship, we carried out acute recordings in anesthetized cats, measuring visual responses and firing rates in layer 2/3 neurons after 1–2 h of post-MD sleep (Fig. 3*E*). We compared mean OD scores for principal neurons at each recording site with average spontaneous firing rates in neighboring FS interneurons (*SI Materials and Methods*). We found that principal neurons showed a greater preference for the open eye at sites where spontaneous activity in neighboring FS interneurons was lowest (Fig. 3*E*). Thus, in recordings from both anesthetized and freely behaving cats, post-MD depression of FS interneuron activity is proportional to ODP. This suggests that disinhibition of glutamatergic circuitry could play an important role in sleep-dependent consolidation of ODP.

Increased Principal Neuron Activity During Post-MD Sleep Is Proportional to OD Plasticity. If principal neurons are disinhibited during post-MD sleep, they should show an increase in firing after MD. We found that principal neuron firing increased during post-MD NREM sleep (Fig. 4*A*), a state that constituted 50–60% of the 6-h post-MD recording period (Fig. S5). This increase was seen relative to both baseline NREM firing and NREM firing in No-MD control cats ($P < 0.05$, two-way ANOVA, Holm–Sidak post hoc test). Furthermore, post-MD plasticity was proportional to firing-rate increases during NREM sleep (Fig. 4*B*). Firing rates in REM sleep were also slightly (but not significantly) increased following MD (Fig. 4*A*), and REM firing-rate increases also correlated with open-eye response potentiation (Fig. 4*B*). In contrast, changes in activity during waking were not related to plasticity measures [not significant (NS), Pearson correlation]. In contrast to firing-rate changes in FS interneurons, firing-rate changes in principal neurons after MD were not related to their baseline ODI (NS, Pearson correlation). These data suggest that increased activity among principal neurons promotes ODP consolidation during sleep.

Sleep-Dependent Plasticity Is Proportional to Phase-Locking of Principal Neuron Firing to NREM Sleep Oscillations. Previous studies have shown that sleep-dependent learning and memory consolidation are associated with changes in cortical activity during NREM sleep, including localized changes in slow waves or sleep spindles (21, 22). These oscillations result from relatively synchronous, rhythmic (i.e., coherent or phase-locked) firing among cortical neurons during NREM sleep (23, 24). Such a pattern of phase-locked firing between pre- and postsynaptic neurons (at lag times of ±50–100 ms) could drive spike-timing–dependent plasticity at excitatory synapses (25). We hypothesized that phase-locked firing during NREM sleep, in conjunction with MD-induced disinhibition of open-eye–biased principal neurons, strengthens postsynaptic responses to open-eye–biased inputs, promoting ODP. To test this, we first assessed the relationship between phase-locked firing during NREM oscillations and ODP. We compared NREM spike-field coherence for individual neurons between baseline and post-MD recording periods. During post-MD sleep, many principal neurons showed increased phase-locking to both slow waves (0.5–4 Hz) and spindle oscillations (7–14 Hz), which was proportional to sleep-dependent plasticity (Fig. 5 *A* and *B*). Importantly, increased phase-locking was also seen after 6 h of waking in No-MD control cats [although this increase did not correlate with changes in visual responses (NS, Pearson correlation)]. Thus, principal neuron firing coherence during NREM oscillations varies as a function of prior wake time, as suggested previously (22).

Post-MD Changes in Firing Phase During Slow Waves Correlate with ODP. It has been postulated that the phase of neuronal firing with respect to NREM oscillations could play an important role in promoting synaptic plasticity (26–28). However, supportive data from cortical circuits undergoing plasticity in vivo are relatively sparse. To address how phase of firing during NREM relates to plasticity, we compared firing phases during NREM oscillations at baseline and following MD (or waking without MD) in principal neurons and FS interneurons (Fig. 5 *C* and *D*). Principal neurons fired near the middle (180°) of "up states," both before and after MD [before: mean firing phase (θ) = 168°, $P = 1.0E$-8; after: θ = 168°, $P = 3.7E$-13, Rayleigh test]. In contrast, after control (No MD) experience, the firing phase of principal neurons shifted forward [before: θ = 183°, $P = 6.2E$-4; after: θ = 137°, $P = 1.7E$-3, Rayleigh test; $P < 0.05$, Watson–Williams test (29), for phase distributions before vs. after]. Thus, the firing phase for principal neurons differed after waking with MD vs. No MD, with principal neuron firing occurring later with respect to slow wave oscillations following MD ($P < 0.001$, Watson–Williams test, corrected for multiple comparisons, for phase distributions after MD vs. after No MD). Although FS interneurons tended to fire with, or just after, principal neurons at baseline (MD: θ = 182°, $P = 8.1E$-4; No MD: θ = 205°, $P = 1.8E$-3, Rayleigh test; NS, Watson–Williams test for FS interneurons vs. principal neurons), their firing phase shifted forward after 6 h of waking, regardless of visual experience (MD: θ = 169°, $P = 1.5E$-3; No MD: θ = 165°, $P = 1.8E$-3, Rayleigh test; $P < 0.05$, Watson–Williams test, for phase distributions before vs. after in both groups). Because there was a phase change in FS interneuron firing after waking under both conditions, this likely reflects prior sleep–wake history, with earlier firing occurring under conditions of increased sleep pressure. In contrast, we conclude that the timing of principal neuron firing varies as a function of waking sensory experience.

Waking experience also altered principal neuron firing-phase distributions during NREM spindle activity (Fig. 5*C*). Principal neurons, which fired primarily near the peak of spindle oscillation up states at baseline (θ = 171°, $P = 5.0E$-5, Rayleigh test), showed a random firing-phase distribution in the first hours of post-MD sleep, with phases for some neurons shifting as much as 180° with respect to baseline (θ = 14°, $P = 0.13$, Rayleigh test).

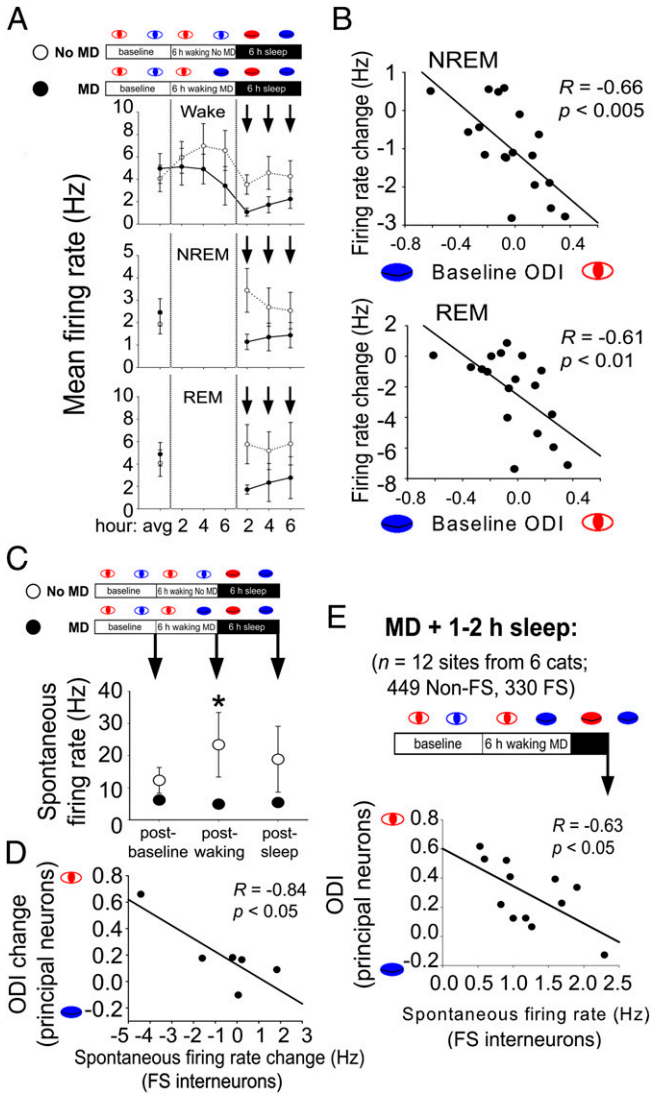

Fig. 3. MD causes overall depression of firing in FS interneurons, which correlates with plasticity during post-MD sleep. (*A*) Mean firing for FS interneurons tended to decrease over the course of MD (relative to No-MD control conditions, filled and open circles, respectively). FS interneuron firing was significantly depressed in all states throughout the post-MD period relative to baseline levels (arrows indicate significant decrease following MD, Holm–Sidak post hoc test), but was transiently enhanced during sleep under No-MD conditions (main effects of visual experience, time, NS; visual experience × time interaction, $F = 7.4$; $P < 0.001$ for NREM; $F = 6.9$; $P < 0.001$ for REM, two-way repeated-measures ANOVA). Data represent mean ± SEM firing rate (in Hz) at each time point throughout recordings. (*B*) FS interneurons biased in favor of the open eye at baseline showed the most profound depression of firing during the first hours of post-MD REM and NREM sleep. (*C*) Spontaneous firing was similarly depressed in FS interneurons during OD testing after MD (relative to No-MD conditions; visual experience × time interaction, $F = 6.5$, $P < 0.005$; an asterisk indicates $P < 0.05$ between MD and No MD, Holm–Sidak test). (*D*) ODI changes in principal neurons during post-MD sleep (averaged across all neurons recorded in each cat) negatively correlated with spontaneous firing-rate changes in neighboring FS interneurons. (*E*) ODIs for principal neurons acutely recorded from anesthetized cats [after 1–2 h of post-MD sleep during the predicted nadir of FS interneuron firing (Fig. 3*A* and Fig. S4)] negatively correlated with spontaneous firing rates in neighboring FS interneurons (data averaged across all neurons at a given cortical site).

Thus, although principal neurons showed greater phase-locking to spindle oscillations after MD, they showed less synchronous firing with respect to one another. Similar phase distribution changes were seen for principal neurons after waking in No-MD cats (Fig. 5*D*). FS interneuron firing showed no clear relationship to spindle oscillations either during baseline or post-MD recording ($P = 0.28$, Rayleigh test at baseline, $P = 0.18$, after MD).

During post-MD slow waves, FS interneuron firing shifts forward with respect to principal neuron firing. We hypothesized that this altered phase relationship might play an important role in plasticity. We found that the greatest principal neuron plasticity occurred in areas of the cortex where FS interneuron firing led principal neuron firing by 60–120° (i.e., roughly 40–300 ms; Fig. 5*E*). Thus, the temporal relationship of firing between FS and principal neurons during slow waves correlates with sleep-dependent plasticity, with earlier FS interneuron firing associated with larger plastic changes. Together with our other present findings, this fact suggests that FS interneurons could play an instructive role in sleep-dependent consolidation of ODP.

Discussion

The current study was designed to assess how waking visual experience and subsequent sleep affect activity and plastic changes in cortical neurons. A previous study by Mioche and Singer recorded visual responses at 4- to 24-h intervals from individual cortical neurons during MD (15). However, the authors did not quantitatively measure vigilance states or distinguish between neurons of different subtypes. Furthermore, because continuous recordings were not carried out between OD tests, it is unclear whether the same neurons were recorded at each test.

By continuously recording neurons through waking experience and subsequent sleep, we show that the earliest detectable changes are in the activity and visual responsiveness of extragranular FS interneurons (summarized in Fig. 5*F*, *Left*). Our present data support spike-timing–dependent plasticity as a hypothetical mechanism whereby inputs from open-eye–biased principal neurons to FS interneurons are depressed during waking MD (Fig. 2). This reduction in excitatory input explains both the observed depression of open-eye visual responses in FS interneurons (Fig. 1) and their observed decrease in firing (primarily in open-eye–biased areas of the cortex; Fig. 3) across waking MD and during post-MD sleep. We hypothesize that depressed FS interneuron firing in open-eye–biased areas of the cortex decreases feedback inhibition to neighboring open-eye–biased principal neurons, which can then drive subsequent plastic changes seen throughout the extragranular layers (Fig. 5*F*, *Right*). In support of this idea, principal neurons show increased firing during post-MD sleep, which is proportional to both sleep-dependent ODP and open-eye response potentiation (Fig. 4*B*). This is consistent with our previous finding of increased multiunit activity in the visual cortex after MD, which is proportional to sleep-dependent ODP (1). Increases in firing in individual principal neurons could result from a decrease in inhibitory input (e.g., from neighboring FS interneurons), an increase in excitatory input (e.g., from disinhibited principal neurons), or both. Future studies will be needed to assess how MD and subsequent sleep affect postsynaptic currents in principal neurons. Enhancement of postsynaptic GABA receptor signaling has been reported in vitro in response to "sleep-like" patterns of activity (30), but it is unclear whether this finding translates to the natural sleep state or how this change in inhibition affects cortical circuit function.

One might expect that increased activity in open-eye–biased principal neurons could promote ODP, regardless of the animal's vigilance state. Thus, a major unresolved issue is, why is sleep required for ODP (1, 2)? More specifically, what unique features of network activity during sleep are essential for ODP? We show that sleep-dependent plasticity among principal neurons is proportional to phase-locking of their firing during NREM sleep oscillations (Fig. 5 *A* and *B*). Importantly, increased phase-locking was also seen after a 6-h period of waking without MD, suggesting that increased principal neuron spike-field coherence in NREM may be a homeostatic response to sleep loss. This finding makes sense in light of the fact that sleep deprivation increases slow wave amplitude (31), which is associated with more synchronous firing

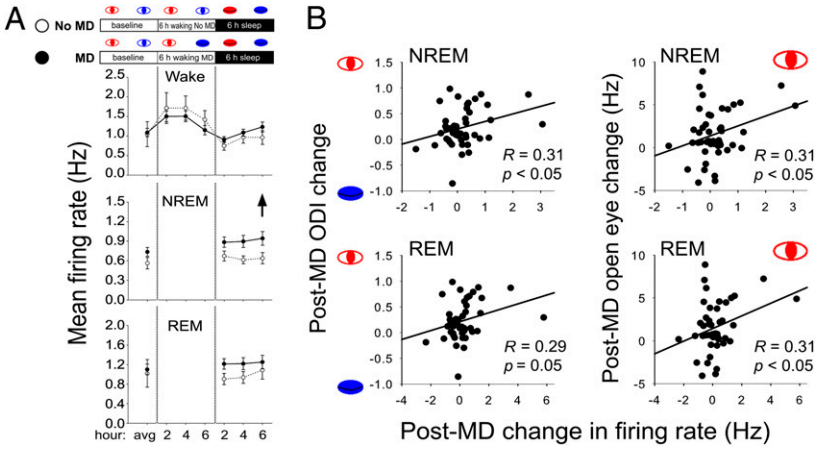

Fig. 4. Principal neurons show increased firing during post-MD sleep. (*A*) Principal neuron activity was comparable during waking experience with or without MD, but increased significantly during post-MD NREM sleep (main effect of visual experience, $F = 4.2$, $P < 0.05$; main effect of time, visual experience × time interaction, NS, two-way repeated-measures ANOVA; arrow indicates significant increase vs. No-MD condition, Holm–Sidak post hoc test). Data represent mean ± SEM firing rate (in Hz) at each time point throughout recordings. (*B*) In principal neurons recorded after MD, firing-rate increases (from baseline) during post-MD NREM sleep correlated with ODI changes and with increases in open-eye response magnitude across the post-MD period. Firing-rate changes in REM sleep also correlated with open-eye response changes.

among cortical neurons (24). Thus, increased phase-locking is not uniquely associated with prior MD. Nonetheless, taken together with our previous finding that ODP correlates with post-MD NREM sleep time (2), our current data suggest that the waves of synchronous network activity that characterize NREM sleep are needed to consolidate ODP.

Firing relationships between FS interneurons and principal neurons were also altered during post-MD slow wave oscillations (Fig. 5*C*). Principal neuron firing, which showed a phase advance under No-MD control conditions, showed no phase change after MD, suggesting that firing phase in this population varies as a function of prior visual experience. In contrast, a general phase

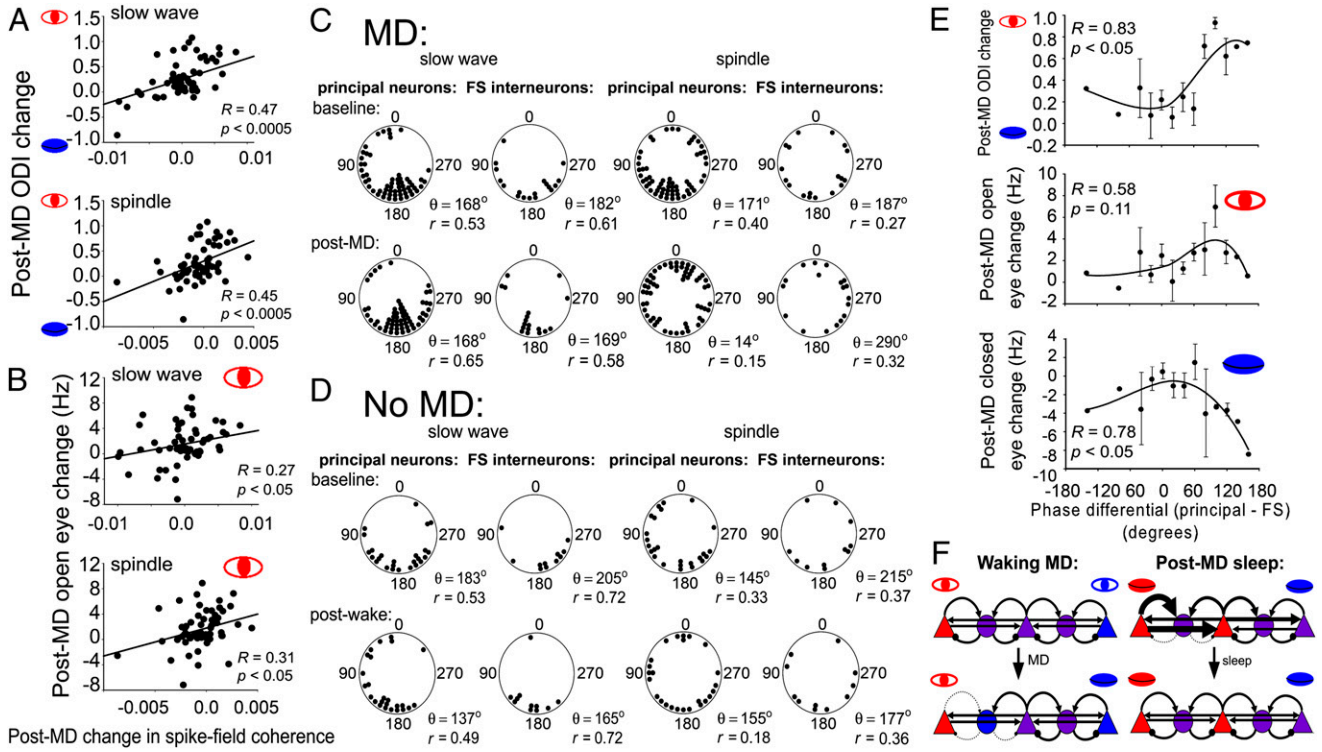

Fig. 5. Changes in principal and FS neuron activity during post-MD NREM oscillations are proportional to plasticity. Post-MD changes in spike field coherence (during both slow wave and spindle oscillations) were proportional both to ODI changes (*A*) and to open-eye response potentiation (*B*) in principal neurons. (*C*) Distributions of mean firing phases relative to local slow wave and spindle oscillations are shown for neurons recorded from all cats at baseline and in the post-MD period. Each point represents one FS or principal neuron with mean spike phase at a given angle. Mean phase angle (θ) and *r* values for each distribution are shown. (*D*) For comparison, firing-phase distributions are shown for neurons recorded under No-MD control conditions. (*E*) Relationships between slow-wave FS interneuron/principal neuron firing-phase differential and post-MD plasticity in principal neurons. Values are based on the differential between firing phases of individual principal neurons and the mean firing phase of FS interneurons recorded on the same stereotrode bundle. For display purposes, data were binned in 20° intervals; mean values (±SEM) for these intervals are shown, together with a third-degree polynomial regression fit to the data points. At sites where FS interneuron firing led principal neuron firing by 60–120° during slow-wave oscillations, post-MD ODI changes in principal neurons were greatest. (*F*) Overview of response changes and hypothesized neural circuit changes during waking MD (*Left*) and post-MD sleep (*Right*). During waking MD, excitatory inputs to FS interneurons from open-eye–biased principal neurons are depressed, leading to decreased firing in these FS interneurons. During post-MD sleep, disinhibition leads to increased output from open-eye–biased principal neurons, which promotes postsynaptic strengthening of open-eye responses (and, thus, open-eye preference) in target neurons.

advance in FS interneuron firing was seen after waking under both MD and No-MD conditions. This suggests that the phase of FS interneuron firing is altered as a function of sleep pressure. Our study describes firing-phase alterations in cortical neurons resulting from sleep homeostasis. However, if the forward advance that we see in FS interneurons (and under control conditions in principal neurons) is a general feature of cortical neuron firing after prolonged waking, it would explain previously reported alterations of cortical network activity associated with sleep homeostasis. For example, previous studies found that increased sleep pressure generally leads to increasingly synchronous firing at the "onset" of each slow wave; at the field potential level, this results in slow waves with steeper initial slopes during early recovery sleep (24).

After MD, shifts in FS interneuron activity with respect to principal neuron activity may have functional significance for consolidating ODP, because the greatest sleep-dependent plasticity occurs where FS interneuron firing leads principal neuron firing by roughly 40–300 ms (Fig. 5*E*). We would predict that 40–300 ms after FS interneurons fire, inhibitory postsynaptic current would still be present in neighboring principal neurons. This time frame is well within the range of decay times reported for inhibitory postsynaptic potentials elicited in principal neurons in response to FS interneuron input in vivo (32) and for inhibitory currents elicited in cortical slices (33). To understand how principal neuron firing under these conditions could promote ODP, we must take into account the initial changes in FS interneuron responsiveness induced by MD. Our data predict that following MD, FS interneuron inhibitory feedback to open-eye–biased principal neurons is reduced, and feedback to closed-eye–biased principal neurons is maintained (Fig. 5*F*). Thus, during NREM slow waves, activity among open-eye–biased principal neurons would be minimally affected by the firing of presynaptic FS interneurons, and closed-eye–biased principal neurons would be inhibited. Under these conditions, input to surrounding neurons from open-eye–biased principal neurons would predominate over closed-eye–biased input (Fig. 5*F*, *Right Top*). Strengthening of excitatory open-eye–biased inputs to FS interneurons during post-MD slow waves would eventually lead to the restoration of binocularity (Fig. 5*F*, *Right Bottom*, and Fig. 1) and the restoration of firing rates to baseline levels (Fig. S4) that we observe in this population. Strengthening open-eye–biased inputs to principal neurons would drive OD shifts across post-MD sleep (Fig. 1) and the progressive increase in principal neuron firing that we observe in the hours after MD (Fig. 4*A*). Taken together, our data suggest that the changes in FS interneurons initiated by waking visual experience play an instructive role in subsequent sleep-dependent consolidation of ODP in the cortex by transiently biasing activity of cortical circuits in favor of open-eye pathways.

Materials and Methods

On postnatal day 20–25 (before the peak of the critical period for ODP), cats were implanted with custom-built, drivable headstages. Each headstage was composed of two bundles seven stereotrodes each placed within the medial bank of the right-hemisphere primary visual cortex.

Signals from each electrode were split and differentially filtered to obtain spike data and local field potential data at each recording site. Individual neurons were tracked throughout an experiment on the basis of spike waveform, relative spike amplitude on the two stereotrode recording wires, neuronal subclass (e.g., FS vs. principal), and orientation preference. Complete materials and methods are in *SI Materials and Methods*.

ACKNOWLEDGMENTS. This work was supported by National Institutes of Health (NIH) Grants R01EY019022 and R01HL114161 (to M.G.F.); and by NIH Grants F32EY017766 and K99EY021503 and a For Women In Science Postdoctoral Fellowship from L'Oréal USA and the American Association for the Advancement of Science (all to S.J.A.).

1. Aton SJ, et al. (2009) Mechanisms of sleep-dependent consolidation of cortical plasticity. *Neuron* 61(3):454–466.
2. Frank MG, Issa NP, Stryker MP (2001) Sleep enhances plasticity in the developing visual cortex. *Neuron* 30(1):275–287.
3. Seibt J, et al. (2012) Protein synthesis during sleep consolidates cortical plasticity in vivo. *Curr Biol* 22(8):676–682.
4. Fagiolini M, et al. (2004) Specific GABAA circuits for visual cortical plasticity. *Science* 303(5664):1681–1683.
5. Fagiolini M, Hensch TK (2000) Inhibitory threshold for critical-period activation in primary visual cortex. *Nature* 404(6774):183–186.
6. Morishita H, Miwa JM, Heintz N, Hensch TK (2010) Lynx1, a cholinergic brake, limits plasticity in adult visual cortex. *Science* 330(6008):1238–1240.
7. Harauzov A, et al. (2010) Reducing intracortical inhibition in the adult visual cortex promotes ocular dominance plasticity. *J Neurosci* 30(1):361–371.
8. He H-Y, Hodos W, Quinlan EM (2006) Visual deprivation reactivates rapid ocular dominance plasticity in adult visual cortex. *J Neurosci* 26(11):2951–2955.
9. Maffei A, Nelson SB, Turrigiano GG (2004) Selective reconfiguration of layer 4 visual cortical circuitry by visual deprivation. *Nat Neurosci* 7(12):1353–1359.
10. Yazaki-Sugiyama Y, Kang S, Câteau H, Fukai T, Hensch TK (2009) Bidirectional plasticity in fast-spiking GABA circuits by visual experience. *Nature* 462(7270):218–221.
11. Trachtenberg JT, Trepel C, Stryker MP (2000) Rapid extragranular plasticity in the absence of thalamocortical plasticity in the developing primary visual cortex. *Science* 287(5460):2029–2032.
12. Yoshimura Y, Callaway EM (2005) Fine-scale specificity of cortical networks depends on inhibitory cell type and connectivity. *Nat Neurosci* 8(11):1552–1559.
13. Otsuka T, Kawaguchi Y (2009) Cortical inhibitory cell types differentially form intralaminar and interlaminar subnetworks with excitatory neurons. *J Neurosci* 29(34):10533–10540.
14. Maffei A, Nataraj K, Nelson SB, Turrigiano GG (2006) Potentiation of cortical inhibition by visual deprivation. *Nature* 443(7107):81–84.
15. Mioche L, Singer W (1989) Chronic recordings from single sites of kitten striate cortex during experience-dependent modifications of receptive-field properties. *J Neurophysiol* 62(1):185–197.
16. Kameyama K, et al. (2010) Difference in binocularity and ocular dominance plasticity between GABAergic and excitatory cortical neurons. *J Neurosci* 30(4):1551–1559.
17. Gandhi SP, Yanagawa Y, Stryker MP (2008) Delayed plasticity of inhibitory neurons in developing visual cortex. *Proc Natl Acad Sci USA* 105(43):16797–16802.
18. Smith GB, Bear MF (2010) Bidirectional ocular dominance plasticity of inhibitory networks: Recent advances and unresolved questions. *Front Cell Neurosci* 4:21.
19. Lu JT, Li CY, Zhao JP, Poo MM, Zhang XH (2007) Spike-timing-dependent plasticity of neocortical excitatory synapses on inhibitory interneurons depends on target cell type. *J Neurosci* 27(36):9711–9720.
20. Thomson AM, West DC, Wang Y, Bannister AP (2002) Synaptic connections and small circuits involving excitatory and inhibitory neurons in layers 2-5 of adult rat and cat neocortex: Triple intracellular recordings and biocytin labelling in vitro. *Cereb Cortex* 12(9):936–953.
21. Huber R, Ghilardi MF, Massimini M, Tononi G (2004) Local sleep and learning. *Nature* 430(6995):78–81.
22. Nishida M, Walker MP (2007) Daytime naps, motor memory consolidation and regionally specific sleep spindles. *PLoS ONE* 2(4):e341.
23. Destexhe A, Contreras D, Steriade M (1999) Spatiotemporal analysis of local field potentials and unit discharges in cat cerebral cortex during natural wake and sleep states. *J Neurosci* 19(11):4595–4608.
24. Vyazovskiy VV, et al. (2009) Cortical firing and sleep homeostasis. *Neuron* 63(6):865–878.
25. Froemke RC, Poo MM, Dan Y (2005) Spike-timing-dependent synaptic plasticity depends on dendritic location. *Nature* 434(7030):221–225.
26. Eschenko O, Magri C, Panzeri S, Sara SJ (2012) Noradrenergic neurons of the locus coeruleus are phase locked to cortical up-down states during sleep. *Cereb Cortex* 22(2):426–435.
27. Sejnowski TJ, Destexhe A (2000) Why do we sleep? *Brain Res* 886(1–2):208–223.
28. Aton SJ, Seibt J, Frank MG (2009) Sleep and memory. *Encyclopedia of Life Sciences*. Wiley, New York. Avaliable at www.els.net, 10.1002/9780470015902.a0021395.
29. Batschelet E (1981) *Circular Statistics in Biology (Mathematics in Biology)* (Academic Press, New York).
30. Kurotani T, Yamada K, Yoshimura Y, Crair MC, Komatsu Y (2008) State-dependent bidirectional modification of somatic inhibition in neocortical pyramidal cells. *Neuron* 57(6):905–916.
31. Knoblauch V, Kräuchi K, Renz C, Wirz-Justice A, Cajochen C (2002) Homeostatic control of slow-wave and spindle frequency activity during human sleep: Effect of differential sleep pressure and brain topography. *Cereb Cortex* 12(10):1092–1100.
32. Gonzalez-Burgos G, Krimer LS, Povysheva NV, Barrionuevo G, Lewis DA (2005) Functional properties of fast spiking interneurons and their synaptic connections with pyramidal cells in primate dorsolateral prefrontal cortex. *J Physiol* 93(2):942–953.
33. Brill J, Huguenard JR (2009) Robust short-latency perisomatic inhibition onto neocortical pyramidal cells detected by laser-scanning photostimulation. *J Neurosci* 29(23):7413–7423.

Supporting Information

Aton et al. 10.1073/pnas.1208093110

SI Materials and Methods

Housing Conditions and Animal Husbandry. All animal husbandry and surgical/experimental procedures were approved by the University of Pennsylvania Institutional Animal Care and Use Committee board for animal care and use. Survival procedures were accompanied by pre- and postoperative care as described previously (1, 2). Unless otherwise noted, cats were kept on a 12 h:12 h light:dark cycle (lights on at 0700 hours) and were given food and water ad libitum.

Implantation of Stereotrode Recording Implants. On postnatal day 20–25 (before the peak of the critical period for ocular dominance plasticity), cats were implanted with custom-built, drivable headstages (EIB-36; Neuralynx) under isoflurane anesthesia. Each headstage was composed of two bundles (each ~200 μm in diameter, spaced 1–2 mm apart) of seven stereotrodes each (25-μm nichrome wire; California Fine Wire) placed within the medial bank of the right-hemisphere primary visual cortex (ipsilateral to the closed eye during MD); reference and ground electrodes (silver-plated copper wire; Alpha Wire) were placed over the left-hemisphere primary visual cortex and cerebellum, respectively, and three electromyography (EMG) electrodes (braided stainless-steel wire; Cooner Wire) were placed deep in the nuchal muscle.

Experimental Design and Recording Procedures. Starting at postnatal day 25–30, cats were placed in a lightproof, illuminated sleep-recording chamber, and headstages were connected to a lightweight cable and commutator to record neural signals. Signals from each electrode were split and differentially filtered to obtain spike data (150 Hz–9 kHz) and local field potential (LFP)/electroencephalographic (EEG) data (0.7 Hz–170 Hz) at each recording site. Data were amplified in two stages (at 20× and 50×), digitized, and recorded at 40 kHz using Plexon MAP hardware and RASPUTIN software (Plexon Inc.).

Stereotrode bundles were advanced into the cortex in 10- to 20-μm steps until stable neuronal recordings (with similar spike waveforms continuously present for >24 h) could be maintained. Once stable recordings were obtained, the headstages were no longer moved unless otherwise indicated.

Day 1 of chronic recordings began with a 6- to 12-h baseline, followed by a 6-h period during which the cats were kept awake (through a combination of gentle handling, novel object exploration, and vocalization) under normal room illumination, starting at 0700–0900 hours. During this 6-h period, a subset of animals ($n = 3$, age 35.7 ± 1.2 d) had normal binocular visual experience (No-MD controls), whereas another group received right-eye MD ($n = 3$). MD was achieved without anesthesia by covering the right eye with an adhesive light-proof patch, as described previously (3). All cats (MD and No MD) were awake for >97% of total recording time during this 6-h window. After the 6-h waking period, cats were allowed to sleep ad libitum in complete darkness for the next 6 h. At intervals (after baseline, after waking visual experience, and after subsequent sleep) cats were gently restrained, as described previously (3), and visual stimuli were presented to the two eyes for OD assessments (see below).

On day 2 of recording, cats who had the control (No MD) visual experience on day 1 underwent MD at the same circadian time (thus total $n = 6$ for MD experiments, age at MD 37.8 ± 1.0 d). In two of these three cats, recordings continued to be collected at the same recording site without advancing the headstage; in the third cat, the headstage position was adjusted downward ~200 μm between No-MD and MD experiments. We did not observe any differences in the effects of MD based on whether a No-MD procedure occurred previously. Recordings of ongoing activity and OD assessments for day 2 were identical to procedures described for day 1.

Lesioning and Laminar Analysis of Recording Sites. At the end of recordings, cats were anesthetized with isoflurane, and all electrode sites were lesioned (2 mA, 3 s per wire). Cats were euthanized and perfused with formalin, after which the visual cortex was postfixed and sectioned at 50 μm for cresyl violet staining. In cases where the two stereotrode recording bundles were localized to different layers ($n = 2$ cats), recording locations for individual neurons were identified based on the anterior–posterior position of the two electrode bundles' lesions.

Nine of 11 recording sites (64/79 neurons) were located in layers 2/3, and the remaining two sites (15/79 neurons) were located in layers 5 and 6 (Fig. S2).

Sleep/Wake Analysis. Intracortical LFP and nuchal EMG signals were used to assign polysomnographic data into periods of rapid eye movement (REM) sleep, non-REM sleep (NREM), and waking states using NeuroExplorer software (Plexon) as described previously (3). The proportion of time spent in REM, NREM, and waking (and mean bout duration for each state) was calculated during the post-MD period using standard conventions (3) (Fig. S5).

Single-Unit Discrimination and Classification. Single-neuron data were discriminated offline using standard principal-component based procedures (Offline Sorter; Plexon; Fig. S1). Neurons were classified as either fast-spiking (FS) interneurons or non–fast-spiking (putative principal) neurons using standard procedures on the basis of their interspike interval (ISI) distribution and spike waveform durations (i.e., width at half-maximal amplitude) (4, 5). FS neurons were characterized by short spike duration (<0.5 ms at half-maximal amplitude) and by a highly regular ISI distribution (without repetitive bursting), peaking at ≤20 ms on average (5, 6) (Fig. S1).

Individual neurons were tracked throughout an experiment on the basis of spike waveform, relative spike amplitude on the two stereotrode recording wires, neuronal subclass (e.g., FS vs. principal), and orientation preference. Neurons that showed large changes (greater than 45°) in preferred orientation during the course of an experiment were excluded from analysis. Within each experiment (No MD or MD), only those neurons that were verifiably recorded throughout the entire experiment (i.e., those that were recorded throughout baseline, visual experience, and subsequent sleep recording) were included in analyses of OD or activity patterns. Because the subsets of neurons stably recorded through the No-MD experiment in a given cat were not necessarily the same set of neurons recorded throughout the subsequent MD experiment, neurons from each experiment were treated separately, even if recorded from the same cat. No repeated-measures statistical comparisons were made across No-MD and MD conditions.

Modified OD Assessments in Freely Behaving Cats. OD testing was carried out in nonanesthetized cats using methods modified from Mioche and Singer (7), as described previously (3). For presentation of visual stimuli during OD testing, cats were lightly restrained at intervals throughout the experiment and positioned 40 cm in front of a 40-inch LCD monitor (Samsung) on which

full-field, slowly drifting, reversing gratings (5 s duration, 0.2 cycles/degree, drifting at 2 cycles/s, reversing at 1 Hz) were displayed. OD assessments were made by covering each of the two eyes with a light-proof patch in a counterbalanced design [i.e., left eye (LE) open, right eye (RE) open, both eyes patched, RE open, LE open, both eyes patched], and a series of oriented gratings were presented (four orientations: 0°, 45°, 90°, 135°, plus blank screen, repeated eight times per eye). The same stimulus set was presented with both eyes patched to assess spontaneous background activity.

Mean firing for each neuron was assessed for each eye and stimulus orientation. At each experimental interval (after baseline, visual experience, or subsequent sleep), LE/RE ratios (i.e., OD scores) were calculated as an ocular dominance index (ODI): ODI = (LE − RE)/(LE + RE), where LE = peak firing-rate response to stimulation of the LE at the preferred stimulus orientation, and RE = peak firing-rate response to stimulation of the LE at the preferred stimulus orientation. Thus, ODIs ranged from −1 (responsive only to RE stimulation) to +1 (responsive only to LE stimulation), with 0 indicating equal responsiveness to stimulation of either eye. To assess changes in response magnitude over time, each neuron's peak LE or RE firing-rate responses were normalized to its mean spontaneous activity (i.e., during trials where both eyes were patched) at each interval. This normalization allowed direct comparisons of visual responses between experimental phases, controlling for nonspecific effects of sleep and wakefulness or other variables such as circadian time on overall neuronal excitability (e.g., in FS cells).

Statistical Measurements. Statistical comparisons were made only for populations of neurons stably recorded across a given experimental period. For these neurons, ODI, normalized LE and RE responses, and spontaneous activity were compared after baseline, after 6 h of waking visual experience, and after 6 h of subsequent sleep using repeated-measures ANOVA on ranks.

Each neuron's firing rate was averaged within each state (i.e., NREM, REM, and wakefulness) across the last 6 h of baseline recording in 2-h bins during visual experience and in 2-h bins during subsequent sleep. Mean firing for FS interneurons and principal neurons was compared across time bins between No-MD and MD conditions using two-way ANOVA (SigmaPlot).

To assess relationships between firing-rate changes and post-MD plasticity, principal neurons and FS interneurons were again considered separately. Activity changes were calculated within each state as (mean firing post-MD − mean firing baseline). Changes in ODI and open-eye/closed-eye responses during sleep were assessed for each neuron as (ODI post sleep − ODI post MD) and (peak response post sleep − peak response post MD), respectively. For correlating changes in FS interneurons and neighboring principal neurons, ODI or mean firing changes were averaged among neurons of the same type (principal or FS) recorded from the same site. For longitudinal recordings, this refers to all of the neurons recorded on the same stereotrode bundle. For acute experiments, this refers to all neurons recorded at a given penetration by the 16-electrode array.

Cross-correlated firing between neurons was quantified using standard procedures and Neuroexplorer software (Plexon). Cross-correlograms were z-scored as shown in Fig. 2 to normalize for effects of overall firing rate on correlation. z-Scored cross-correlated firing was summed for each principal neuron–FS neuron pair between a −10- and 10-ms lag [where spike timing-dependent plasticity produces the most pronounced depression in principal neuron–FS interneuron synapses, as described previously (8)] during waking at baseline (before MD) and during the first hour of MD to calculate the MD-associated change in correlated firing shown in Fig. 2*C*. Each value in Fig. 2*C* represents the mean of cross-correlated firing changes (and the mean baseline ODI differential) between a single FS interneuron and all principal neurons recorded on the same stereotrode bundle.

Spike-field coherence was calculated for each neuron with respect to LFP signal on the same stereotrode wire. LFP signals were bandpass-filtered in either slow wave (0.5–4 Hz, second-order Butterworth) or spindle (7–14 Hz, fifth-order Butterworth) frequency bands. Mean coherence for each neuron was quantified across baseline NREM recording and in 1-h bins across the post-MD period, and changes in coherence were quantified as the difference in amplitude (between post-MD and baseline periods) for spike-triggered average oscillations. Increased coherence during slow wave activity was maintained, and correlated with plasticity, throughout the 6-h post-MD sleep period. In contrast, the relationship between spindle-frequency coherence changes and plasticity was present only in the first 2 h of post-MD sleep. For phase analysis, the phase angle of each neuron's spike timing with respect to spike-triggered average oscillation was quantified, using the peak and trough of the oscillation (corresponding to trough and peak of surface EEG oscillations, respectively) as phase markers designated 0° and 180°. Rayleigh test r and θ values were calculated separately for principal and FS neurons across all cats at each time point (at baseline or after MD) using standard circular statistical methods (9). Phase differential was calculated between each principal neuron and the average phase (θ) of FS interneurons recorded on the same stereotrode bundle, both at baseline and during post-MD sleep. Positive-phase differential values (+0–180°) indicated principal neurons that fired after FS interneurons during slow wave oscillations. Mean phase differential values were correlated with plasticity measures in principal neurons across the post-MD period. For display purposes, phase differential values are plotted linearly (Fig. 5*E*). However, statistical results are reported for a standard circular–linear correlation test. Data are binned at 20° intervals for display (Fig. 5*E*); however, statistics were calculated using data from each individual principal neuron.

Similar analyses of spike-field coherence and spike phase were carried out for REM sleep. There was a significant correlation between post-MD increases in coherence during REM gamma (25–100 Hz) oscillations and post-MD ODI changes (in the third and fourth hour post MD) and open-eye response changes (in the fifth and sixth hour) in principal neurons ($P < 0.05$, Pearson correlation). However, there was no clear relationship between spike phase during REM gamma oscillations and plasticity.

Waking experience (MD and No MD) affected FS interneuron coherence in a manner similar to its effects on overall firing rates. During post-MD NREM sleep, FS interneurons showed decreased phase-locking to both slow wave and spindle oscillations, while phase-locking increased after waking in No-MD control cats. However, these changes were not associated with plasticity (not significant, Pearson correlation) and likely reflected differences in FS interneuron firing rates under the two conditions.

Acute Visual Cortex Recordings from Anesthetized Cats. To verify the relationship between OD plasticity and FS interneuron firing-rate changes, six cats (age = 32.3 ± 1.1 d) had their right eyes sutured under isofluorane anesthesia, were kept awake as described above for 6 h of MD, and then were allowed 1–2 h of subsequent ad libitum sleep in total darkness. They were then prepared for microelectrode recordings of single visual cortex neurons under Nembutal anesthesia as described previously (3). Neuronal responses to grating stimuli presented in either eye were recorded extracellularly using a 1- × 1-mm array of 16 electrodes (Frederick Haer). For each set of neurons recorded, eight full-field, slowly drifting, reversing gratings (0.2 cycles/degree, 5-s presentation) were presented randomly to each eye four times (4 × 8 different orientations at 22.5° intervals + blank screen per eye).

Single-neuron data were discriminated offline, neurons were classified as either FS or principal neurons, and ODI and spon-

taneous firing rate (during blank screen presentation) were calculated for each neuron, as described above for chronic recordings.

As was true for our previous studies (2), the use of the 16-electrode array precluded electrode path reconstruction because multiple passes with the array left the cortex too fragile for accurate histological assessment using standard procedures. However, a comparison of the depth of neuronal recordings based on electrode placement (measured in 100-μM steps from the pial surface) provided an estimate of median depth of the recordings (25th and 75th percentile) of 400 μM (200 and 500 μM), indicating that the majority of recorded neurons resided in cortical layer 2/3.

1. Frank MG, Issa NP, Stryker MP (2001) Sleep enhances plasticity in the developing visual cortex. *Neuron* 30(1):275–287.
2. Jha SK, et al. (2005) Sleep-dependent plasticity requires cortical activity. *J Neurosci* 25(40):9266–9274.
3. Aton SJ, et al. (2009) Mechanisms of sleep-dependent consolidation of cortical plasticity. *Neuron* 61(3):454–466.
4. Nowak LG, Azouz R, Sanchez-Vives MV, Gray CM, McCormick DA (2003) Electrophysiological classes of cat primary visual cortical neurons in vivo as revealed by quantitative analyses. *J Neurophysiol* 89(3):1541–1566.
5. Vyazovskiy VV, et al. (2009) Cortical firing and sleep homeostasis. *Neuron* 63(6): 865–878.
6. Azouz R, Gray CM, Nowak LG, McCormick DA (1997) Physiological properties of inhibitory interneurons in cat striate cortex. *Cereb Cortex* 7(6):534–545.
7. Mioche L, Singer W (1989) Chronic recordings from single sites of kitten striate cortex during experience-dependent modifications of receptive-field properties. *J Neurophysiol* 62(1):185–197.
8. Lu JT, Li CY, Zhao JP, Poo MM, Zhang XH (2007) Spike-timing-dependent plasticity of neocortical excitatory synapses on inhibitory interneurons depends on target cell type. *J Neurosci* 27(36):9711–9720.
9. Fisher NI (1993) *Statistical Analysis of Circular Data* (Cambridge Univ Press, Cambridge, UK).

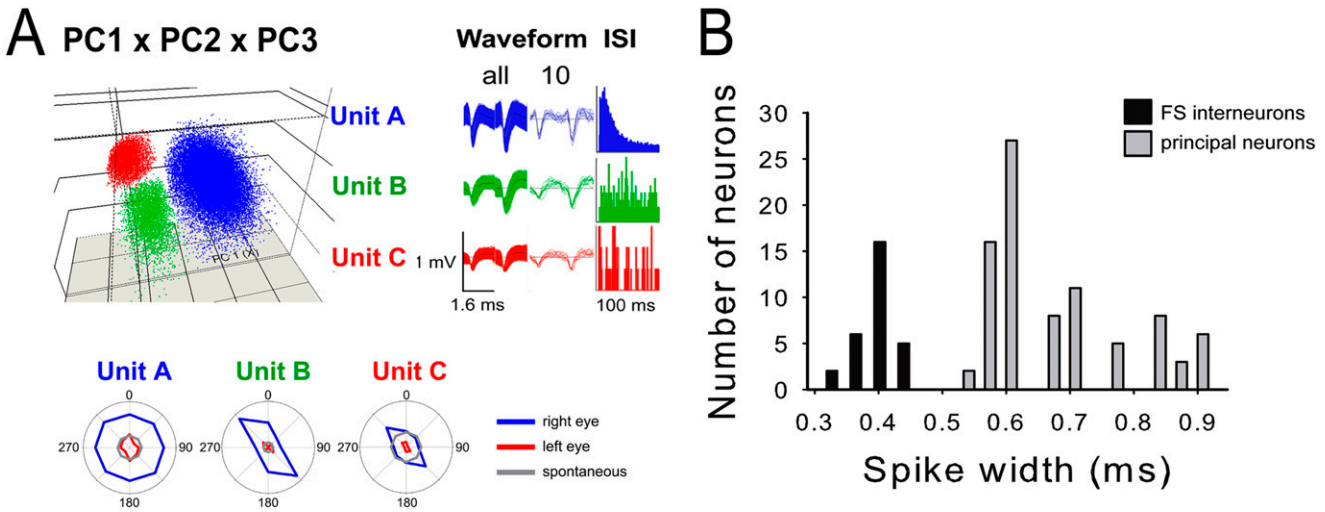

Fig. S1. Properties of FS interneurons and pyramidal neurons in the visual cortex. (*A*) Spike data from three representative neurons [one FS (Unit A) and two principal (Units B and C) neurons] recorded on a single stereotrode. (*Upper Left*) Clusters of spike waveforms from the three neurons in three-dimensional principal component (PC) space. (*Upper Right*) Spike waveforms and interspike interval (ISI) distributions for each neuron. (*Lower*) Baseline visual responses to gratings of various orientations, presented to the left and right eyes, and spontaneous firing-rate responses for each neuron. Note that eye preference and orientation preference is similar in the three neurons, although orientation tuning for the FS neuron is broader than that of the principal neurons, as described previously (1, 2). (*B*) Spike width histogram showing segregation of FS interneuron and principal neuron populations on the basis of spike duration.

1. Nowak LG, Sanchez-Vives MV, McCormick DA (2008) Lack of orientation and direction selectivity in a subgroup of fast-spiking inhibitory interneurons: Cellular and synaptic mechanisms and comparison with other electrophysiological cell types. *Cereb Cortex* 18(5):1058–1078.
2. Kuhlman SJ, Tring E, Trachtenberg JT (2011) Fast-spiking interneurons have an initial orientation bias that is lost with vision. *Nat Neurosci* 14(9):1121–1123.

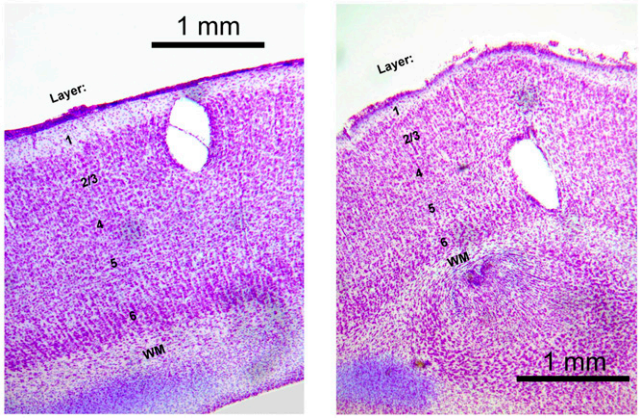

Fig. S2. Representative recording sites showing lesions in layer 2/3 and layers 5 and 6. Lesions are shown in cresyl violet-stained sections of primary visual cortex. The lesion on the left (layer 2/3) is representative of 9 of the 11 recording sites; the lesion on the right (layers 5 and 6) is representative of the remaining two sites.

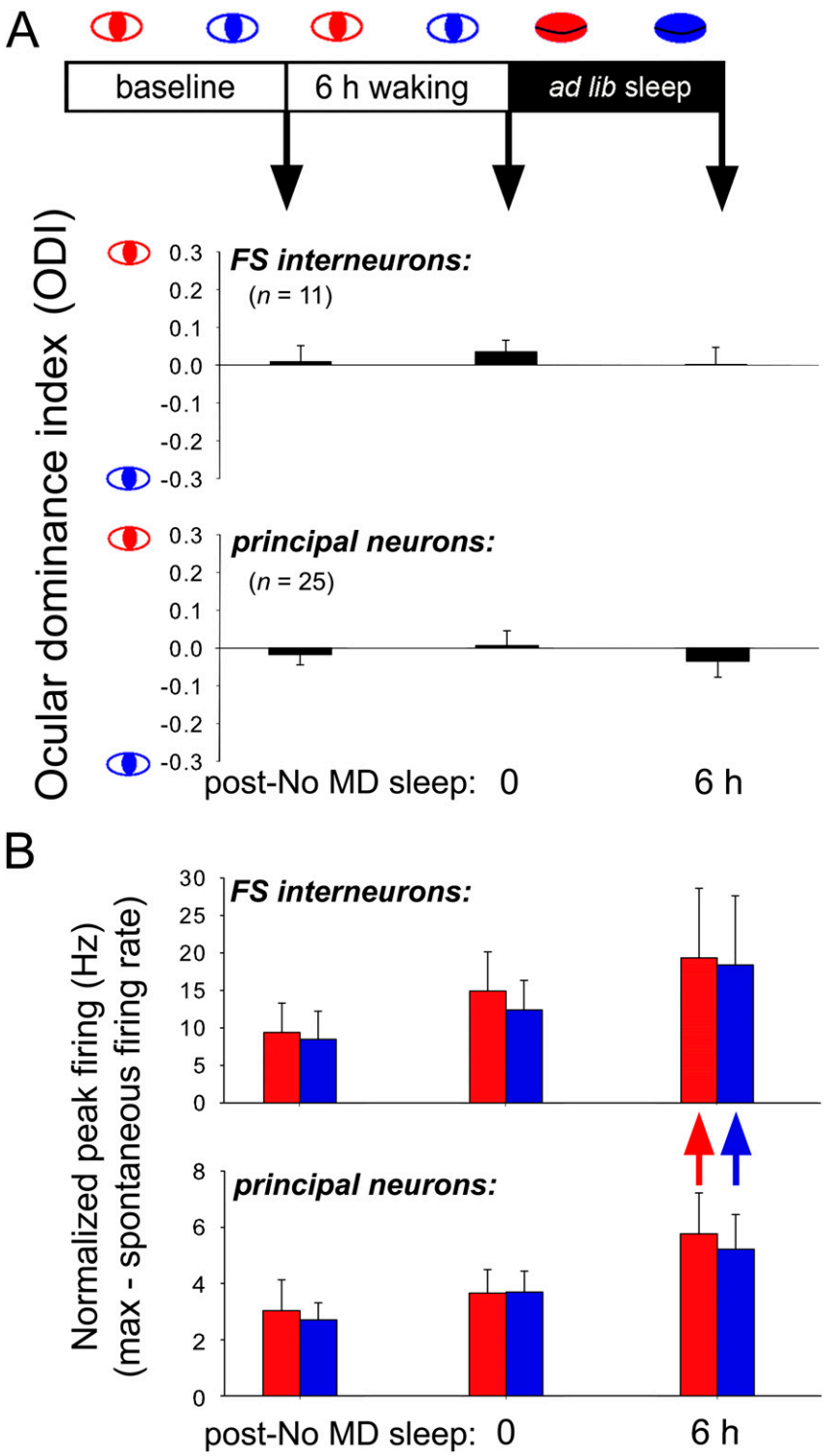

Fig. S3. Changes in ODI and visual responses in cortical neurons during waking without MD and subsequent sleep. ODI values (*A*) were unaltered in both principal and FS neurons across No-MD experiments, although visual responses for both left and right eyes were enhanced in principal neurons after 6 h of ad libitum sleep (*B*; arrows indicate $P < 0.05$ vs. baseline, repeated measures ANOVA).

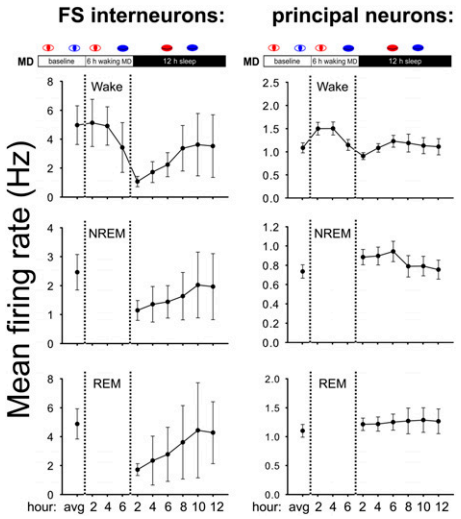

Fig. S4. MD-induced changes in FS interneuron activity are transient. Mean (±SEM) firing rates (in 2-h bins) of FS interneurons recorded from three cats in which the same neuronal populations were stably recorded during baseline, waking MD, 6 h of subsequent sleep (in complete darkness), and continued MD over the next 6 h. Depression of FS neuronal activity (relative to baseline) was transient, with firing rates returning to baseline levels within 6–8 h after the 6-h waking-MD period.

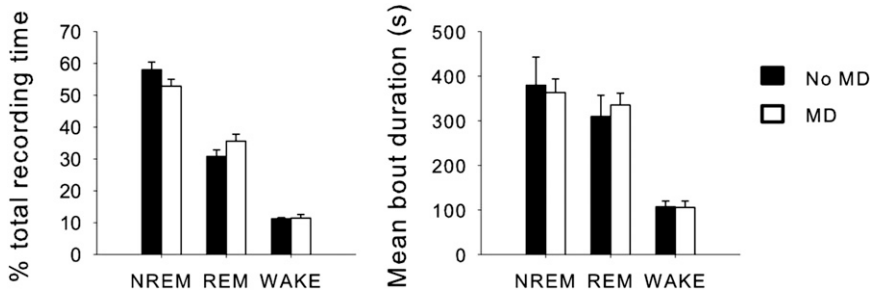

Fig. S5. Sleep amounts and architecture following waking experience. Percentage of total recording time spent in NREM sleep, REM sleep, and wake states and mean bout duration for each state (±SEM), during post-MD and post–No-MD sleep.